0022-3565/09/3282-504–515$20.00
THE JOURNAL OF PHARMACOLOGY AND EXPERIMENTAL THERAPEUTICS
JPET 328:504–515, 2009

Vol. 328, No. 2
144576/3426311
Printed in U.S.A.

Effect of Novel Negative Allosteric Modulators of Neuronal Nicotinic Receptors on Cells Expressing Native and Recombinant Nicotinic Receptors: Implications for Drug Discovery

Tatiana F. González-Cestari, Brandon J. Henderson, Ryan E. Pavlovicz, Susan B. McKay, Raed A. El-Hajj, Aravinda B. Pulipaka, Crina M. Orac, Damon D. Reed, R. Thomas Boyd, Michael X. Zhu, Chenglong Li, Stephen C. Bergmeier, and Dennis B. McKay

Divisions of Pharmacology (T.F.G.-C., B.J.H., S.B.M., R.A.E., D.B.M.) and Medicinal Chemistry and Pharmacognosy (R.E.P., C.L.), College of Pharmacy, The Ohio State University, Columbus, Ohio; Department of Neuroscience, The Ohio State University, College of Medicine and Public Health, Columbus, Ohio (R.T.B., M.X.Z.); and Department of Chemistry and Biochemistry, Ohio University, Athens, Ohio (A.B.P., C.M.O., D.D.R., S.C.B.)

Received August 14, 2008; accepted October 7, 2008

ABSTRACT

Allosteric modulation of nAChRs is considered to be one of the most promising approaches for drug design targeting nicotinic acetylcholine receptors (nAChRs). We have reported previously on the pharmacological activity of several compounds that seem to act noncompetitively to inhibit the activation of $\alpha3\beta4^*$ nAChRs. In this study, the effects of 51 structurally similar molecules on native and recombinant $\alpha3\beta4$ nAChRs are characterized. These 51 molecules inhibited adrenal neurosecretion activated via stimulation of native $\alpha3\beta4^*$ nAChR, with IC_{50} values ranging from 0.4 to 13.0 μM. Using cells expressing recombinant $\alpha3\beta4$ nAChRs, these molecules inhibited calcium accumulation (a more direct assay to establish nAChR activity), with IC_{50} values ranging from 0.7 to 38.2 μM. Radiolabeled nAChR binding studies to orthosteric sites showed no inhibitory activity on either native or recombinant nAChRs. Correlation analyses of the data from both functional assays suggested additional, non-nAChR activity of the molecules. To test this hypothesis, the effects of the drugs on neurosecretion stimulated through non-nAChR mechanisms were investigated; inhibitory effects ranged from no inhibition to 95% inhibition at concentrations of 10 μM. Correlation analyses of the functional data confirmed this hypothesis. Several of the molecules (24/51) increased agonist binding to native nAChRs, supporting allosteric interactions with nAChRs. Computational modeling and blind docking identified a binding site for our negative allosteric modulators near the orthosteric binding site of the receptor. In summary, this study identified several molecules for potential development as negative allosteric modulators and documented the importance of multiple screening assays for nAChR drug discovery.

Several physiological functions involve neuronal nicotinic receptors (nAChRs), including memory and learning, attention, pain perception, and body temperature regulation. In addition, nAChRs may be linked to several disease states, including nicotine addiction, epilepsy, Parkinson's disease, and Alzheimer's disease. Progress in this area is slowed by the lack of pharmacological tools to investigate nAChR involvement in these processes. Most drug discovery programs target the orthosteric site of nAChRs where agonists and competitive antagonists bind (e.g., Dwoskin and Crooks, 2001). Our laboratory is targeting negative allosteric (noncompetitive) sites as a novel approach for nAChR drug discovery. A large number of chemically diverse drugs have been classified as noncompetitive antagonists and are believed to bind to specific sites on nAChRs (Lloyd and Williams, 2000; Arias et al., 2006). Noncompetitive antagonists inhibit nAChR function either by binding allosteric sites and changing conformational states of the receptor (negative allosteric modulators) or by directly blocking the receptor-associated ion channel (ion channel blockers). Several noncompetitive antagonist binding sites have been proposed (Lloyd and Williams, 2000; Arias et al., 2006). One of these sites is located within the nAChR ion channel, in which ligands cause steric

This work was supported in part by National Institutes of Health [Grant DA12707].
Article, publication date, and citation information can be found at http://jpet.aspetjournals.org.
doi:10.1124/jpet.108.144576.

ABBREVIATIONS: nAChR, neuronal nicotinic acetylcholine receptor; MLA, methyllycaconitine; NAM, negative allosteric modulator; AM, acetoxymethyl ester; HEK, human embryonic kidney; LBD, ligand binding domain; MD, molecular dynamics.

blockade. Allosteric sites have been described in the receptor vestibule, in the αM1 domain, or simply as locations at the lipid-protein interface.

Most drug discovery programs focus on the development of agonists and competitive antagonists that target the nAChR orthosteric site. One potential difficulty in this approach is the physiochemical resemblance of orthosteric sites among subtypes of nAChRs. Another approach that could potentially be a powerful tool for therapeutic intervention is the design of drugs that act as allosteric modulators of receptors. Allosteric modulators exist for a variety of receptors (Wess, 2005). Allosteric modulation of nAChRs is considered to be one of the most promising approaches in ligand design for nAChR research and therapeutics (Cassels et al., 2005; Iorga et al., 2006), and the characterization and localization of these sites are beginning to be elucidated (Costa et al., 2003; Iorga et al., 2006; McKay et al., 2007).

Our laboratory has reported previously the synthesis and preliminary characterization of several noncompetitive antagonists of nAChRs that are structurally related to methyllycaconitine (MLA) (Bergmeier et al., 1999, 2004; Bryant et al., 2002; Huang et al., 2008) and has recently described a pharmacophore for the binding site of these molecules (McKay et al., 2007). In the present study, a novel class of negative allosteric modulators (NAMs) of nAChRs is identified and characterized. The following experiments characterize the nature of the inhibitory activities of our NAMs, describe their structure-activity relationships, and define a potential ligand binding domain of these NAMs on α3β4 nAChRs using homology modeling and blind docking approaches.

Materials and Methods

Materials. (−)-Nicotine hydrogen tartrate, α-bungarotoxin, polyethylenimine, and components of N2+ media were obtained from the Sigma-Aldrich (St. Louis, MO). Fluo-4-acetoxymethyl ester (AM), probenecid, and Pluronic F-127 were obtained from Invitrogen (Carlsbad, CA). Dulbecco's modified Eagle's medium, Dulbecco's modified Eagle's medium/F-12 (used in N2+ medium), minimum essential medium, penicillin, streptomycin, and L-glutamine were obtained from Invitrogen. (±)-[5,6-bicycloheptyl-^{3}H]epibatidine (specific activity, 55.5 Ci/mmol) and DL-[7-^{3}H(N)]norepinephrine hydrochloride (specific activity, 10.9 Ci/mmol) were purchased from PerkinElmer Life and Analytical Sciences (Boston, MA). Bovine adrenal glands were purchased from the Herman Falter Packing Company (Columbus, OH). Whatman GF/B filters were purchased from Brandel Inc. (Gaithersburg, MD). All other reagents were purchased from Thermo Fisher Scientific (Waltham, MA). In general, molecules (Fig. 1) were prepared by reaction of hydroxymethyl piperidine with the appropriate alkyl halide to provide the *N*-alkyl hydroxymethyl piperidine, as reported previously by our laboratory (Bergmeier et al., 1999, Bergmeier et al., 2004; Huang et al., 2008). This molecule was then coupled to the appropriate carboxylic acid to provide the target molecule (Bergmeier et al., 2004). All molecules were >98% pure as shown by ^{1}H NMR, ^{13}C NMR, and high-resolution mass spectrometry. Before pharmacological studies, all compounds were converted to their hydrochloride or oxalate salts.

Neurosecretion Studies. Bovine adrenal chromaffin cells were dissociated from intact glands and placed into culture, as described previously by our laboratory (Wenger et al., 1997). A [^{3}H]norepinephrine assay was used to monitor neurosecretion from cultured cells (Wenger et al., 1997). Cells were pretreated for 15 min with the drug before stimulation (10 μM nicotine or 56 mM KCl) in the continued presence of the drug. The concentration of nicotine used in this neurosecretion assay (10 μM) is the EC_{100} value of nicotine (Wenger et al., 1997). When KCl was used as a stimulant, the NaCl concentration in the buffer was reduced accordingly to maintain isotonicity. Cultured adrenal chromaffin cells were typically used 3 to 7 days after isolation.

[^{3}H]Epibatidine Binding to Native and Recombinant α3β4 nAChRs. Membrane preparations from bovine adrenal medullary tissues or HEK 293 cells stably expressing bovine α3β4 nAChRs (BMα3β4 cells) were prepared, and binding assays were performed, as described previously by our laboratory (Free et al., 2003). Briefly, membranes were incubated at room temperature for 60 min in buffer containing 1 nM [^{3}H]epibatidine. Nonspecific binding was determined in the presence of 300 μM nicotine. Specific binding was typically 1 to 2% of total binding for recombinant nAChRs and 5 to 10% for native nAChRs. For homologous competition binding experiments on adrenal membranes, epibatidine was used at increasing concentrations in the presence or absence of 10 μM APB-8. Typically, single concentrations of our molecules (10 μM) were used, except in concentration-response experiments.

Measurement of Intracellular Calcium Using HEK 293 Cells Stably Expressing Recombinant nAChRs. For the calcium accumulation assays, KXα3β4R2 cells (Xiao et al., 1998), which express rat α3β4 nAChRs, were used because functional responses produced by BMα3β4 cells were not as robust as needed for concentration-response studies. Cells were plated on clear poly-D-lysine-coated 96-well plates at a density of 1.2 to 1.5 × 10^5 cells per well and incubated at 37°C in 5% CO_2, using minimum essential medium supplemented with 10% fetal bovine serum, 10 mM L-glutamine, 0.7 mg/ml Geneticin (G418), 100 units/ml penicillin, and 100 μg/ml streptomycin. Forty-eight hours after plating, the cells were washed with HEPES-buffered Kreb's saline (HBK) (155 mM NaCl, 4.6 mM KCl, 1.2 mM $MgSO_4$, 1.8 mM $CaCl_2$, 6 mM glucose, and 20 mM HEPES, pH 7.4) by flicking the plate and loaded for 1 h at 24°C (protected from light) with 40 μl of HBK containing 2 μM fluo-4-AM solution, 2.5 mM probenecid, and 0.05% Pluronic F-127. Fluo-4-AM and Pluronic F-127 were dissolved in dimethyl sulfoxide [100 and 20% (w/v), respectively], resulting in a final dimethyl sulfoxide concentration of <0.1%. At the end of the incubation period, the cells were washed, and 80 μl of the corresponding buffers was added to each well. The fluorescence was measured at ~0.7-s intervals using a fluid handling integrated fluorescence plate reader (Flex Station; Molecular Devices, Sunnyvale, CA).

nAChR antagonism was assessed using the following protocol. For the nicotine control group, HBK (40 μl) was added, and the fluorescence was measured for 40 s. Subsequently, nicotine (40 μl of a 400 μM solution) was added to achieve a final concentration of 100 μM (EC_{100}; see Fig. 3A), and the fluorescence was measured for 60 s. Treatment groups received the antagonist (40 μl of a 3× solution), in the first addition, and then the same nicotine solution (400 μM) with the desired concentration of the antagonist, in the second addition. Sham-treated groups (nonstimulated groups) were treated only with HBK both times. Probenecid (2.5 mM) was included in all of the solutions once the cells were loaded to prevent the leakage of fluo-4 from cells. The fluo-4 fluorescence was read at excitation of 494 nm and emission of 520 nm from the bottom of the plate. Responses were quantified by first calculating the net fluorescence, that is, the difference between stimulated groups' fluorescence values (nicotine control and treatment groups) and sham-treated group fluorescence values. Peak fluorescence values (after stimulation) were obtained. Results were expressed as a percentage of peak values of nicotine-stimulated controls.

To assess nAChR agonist activity, cells were treated with 80 μl of a 2× solution in HBK of the desired concentrations of nicotine or epibatidine. Fluorescence was recorded for 20 s before the stimulation, and 100 s after the stimulation. Sham-treated group (nonstimulated group) received only HBK. Peak fluorescence values were determined after subtraction of sham group's fluorescence values. The percentages of the effects of each concentration of nicotine or epiba-

tidine were calculated in relationship with the effect of 100 μM nicotine or 1 μM epibatidine, respectively.

Homology Modeling and Docking. A homology model of the rat α3β4 ligand binding domain (LBD) was constructed to computationally probe for potential noncompetitive antagonist binding sites. Crystal structures for three molluskan species of homopentameric acetylcholine binding proteins (Celie et al., 2004, 2005; Hansen et al., 2005), along with the mouse α1 LBD monomer (Dellisanti et al., 2007), were used as templates for the modeling process. Models were built in an iterative manner with MODELLER9v1 (Andrej Sali, San Francisco, CA) in which successive rounds focused on refining particular loop regions of the LBD while incorporating the lowest energy model from the previous iteration as an additional template. Model energies were evaluated in the AMBER suite of programs (University of California, San Francisco, CA) in which after explicit water energy minimization, a generalized Born method was used to estimate the free energy of solvation for the 200 models built in each iteration. The internal energy and solvation free energy of each model were summed, and the model with the lowest total energy was chosen as the conformation to which the antagonists were docked.

The relaxed complex method (Lin et al., 2003) coupled with a blind docking approach was used to search for noncompetitive antagonist sites on the final α3β4 LBD model. In the relaxed complex method, docking to different protein conformations as extracted from a molecular dynamics (MD) simulation enhances the probability of reproducing a correct binding mode by taking into consideration the dynamic movements of the receptor. An explicit water MD simulation of the α3β4 model was carried out in AMBER 9 (University of California, San Francisco, CA), and trajectory snapshots were extracted at 200-ps intervals for docking. Blind docking grids were 93.75 × 93.75 × 71.25 Å, with a grid point spacing of 0.375 Å. This encompassed the entire LBD except for the loops that would normally come into contact with the membrane. Following grid construction, the two stereoisomers of COB-3 were docked with AutoDock 4 (The Scripps Research Institute, Jupiter, FL). In all docking runs, compounds were docked 100 times with 100 million energy evaluations, allowing all bonds to rotate freely. Antagonists were docked to a ternary complex in which epibatidine was present in both agonist binding sites to search for noncompetitive binding sites. After docking the two COB-3 stereoisomers, the results for each compound were clustered according to their centroid, with a tolerance of 4 Å. The top four clusters of the each compound at each snapshot were then clustered together to identify consensus docking positions.

Calculations and Statistics. Results were calculated from the number of observations (n) performed in duplicate, triplicate, or quadruplicate. Curve fitting was performed by Prism software (GraphPad Software Inc., San Diego, CA) using the following equation for a single-site sigmoidal dose-response curve with a variable slope: $Y = 100/\{1 + 10[(\log IC_{50} - X) \times HS]\}$, where Y is the percentage of the maximal effect at a given concentration (X), and HS is the Hill coefficient. IC_{50} values and Hill coefficients were obtained by averaging values generated from each individual concentration-response curve. For a few molecules, the IC_{50} values were extrapolated since 50% inhibition was not achieved at the highest concentration used (10 μM); higher concentrations could not be tested due to solubility problems. For these molecules, extrapolated IC_{50} values, as well as the corresponding Hill coefficients, were taken from the mean curve. Results were expressed as arithmetic means ± S.E.M. ($n \geq 3$) or S.D. ($n = 2$), except for IC_{50} and EC_{50} values, which were expressed as geometric means (95% confidence limits).

Results

In this study, a variety of techniques and approaches were used to identify the sites and mechanisms of action of the 51 molecules. The chemical structures of these molecules are found in Fig. 1. Initially, the effects of the drugs on nicotine-stimulated adrenal neurosecretion were investigated. As illustrated in Fig. 2 and Table 1, the drugs inhibited adrenal neurosecretion stimulated using 10 μM nicotine, with IC_{50} values ranging from 0.4 to 13.0 μM. Hill coefficients varied from −1.2 to −5.1. None of the molecules showed agonist activity (data not shown).

The site of action of these molecules for their inhibitory effects on nAChR-stimulated neurosecretion cannot be established using this functional paradigm since multiple steps are involved in the stimulus-secretion coupling pathway. To investigate whether these molecules act via direct interaction with nAChRs, calcium accumulation assays were performed using cells expressing recombinant nAChRs. For this assay, the functional responses (i.e., increases in intracellular calcium) are directly linked to nAChR activation (Stauderman et al., 1998; Chavez-Noriega et al., 2000). For these studies, an HEK 293 cell line stably expressing rat α3β4 nAChRs (KXα3β4R2) was used (Xiao et al., 1998). Table 2 established the feasibility of using this cell line. The relative potencies of nicotine, epibatidine, and one of our own antagonists, COB-2, were identical to values reported in the literature for native bovine adrenal nAChRs (McKay and Trent-Sanchez, 1990; McKay and Burkman, 1993; Wenger et al., 1997; McKay et al., 2007); native nAChRs showed slightly higher apparent affinities for the agonists. The inhibitory effects of the competitive antagonist tubocurarine and the noncompetitive antagonists mecamylamine and tetracaine were also compared (Table 2); no major differences were seen between native bovine and recombinant rat nAChRs. The functional responses of KXα3β4R2 cells were also compared with those of BMα3β4 cells (Fig. 3). For these studies, the calcium concentration in the buffer for BMα3β4 cells was increased to 20 mM to obtain a more robust response (Chavez-Noriega et al., 2000; Pacheco et al., 2001). The concentration-dependent effects of nicotine, tubocurarine, and tetracaine were identical (Fig. 3, A, C, and E), and recombinant bovine nAChRs showed slightly lower apparent affinities for epibatidine, mecamylamine, and COB-2 (Fig. 3, B, D, and F).

The concentration-response effects of the 51 molecules (Fig. 1) on nAChR-stimulated calcium accumulation in KXα3β4R2 cells are found in Fig. 4. All 51 molecules produced concentration-dependent inhibition of nicotine-stimulated increases in $[Ca^{2+}]_i$, with IC_{50} values ranging from 0.7 to 38.2 μM (Fig. 4). These data documented direct antagonist activity of the molecules on nAChRs. Hill coefficients ranged from −0.6 to −2.0; these values were not significantly different from −1.0 (unpaired t test, p values >0.05). None of these molecules showed any agonist activity (data not shown).

When the effects of the inhibitors on native and recombinant nAChRs were directly compared via Pearson analysis, no correlation was demonstrated (Pearson $r = -0.176$, $p = 0.217$) (Fig. 5). One possibility involves the neurosecretion assay; the inhibitors may have additional effects on more distal steps (downstream of nAChR activation) of the stimulus-secretion coupling pathway. To address this hypothesis, the effects of the drugs on neurosecretion stimulated using depolarizing concentrations of KCl (56 mM) were investigated. This method of stimulation bypasses activation of nAChRs and directly depolarizes adrenal membranes, resulting in neurosecretion. This approach has been used to local-

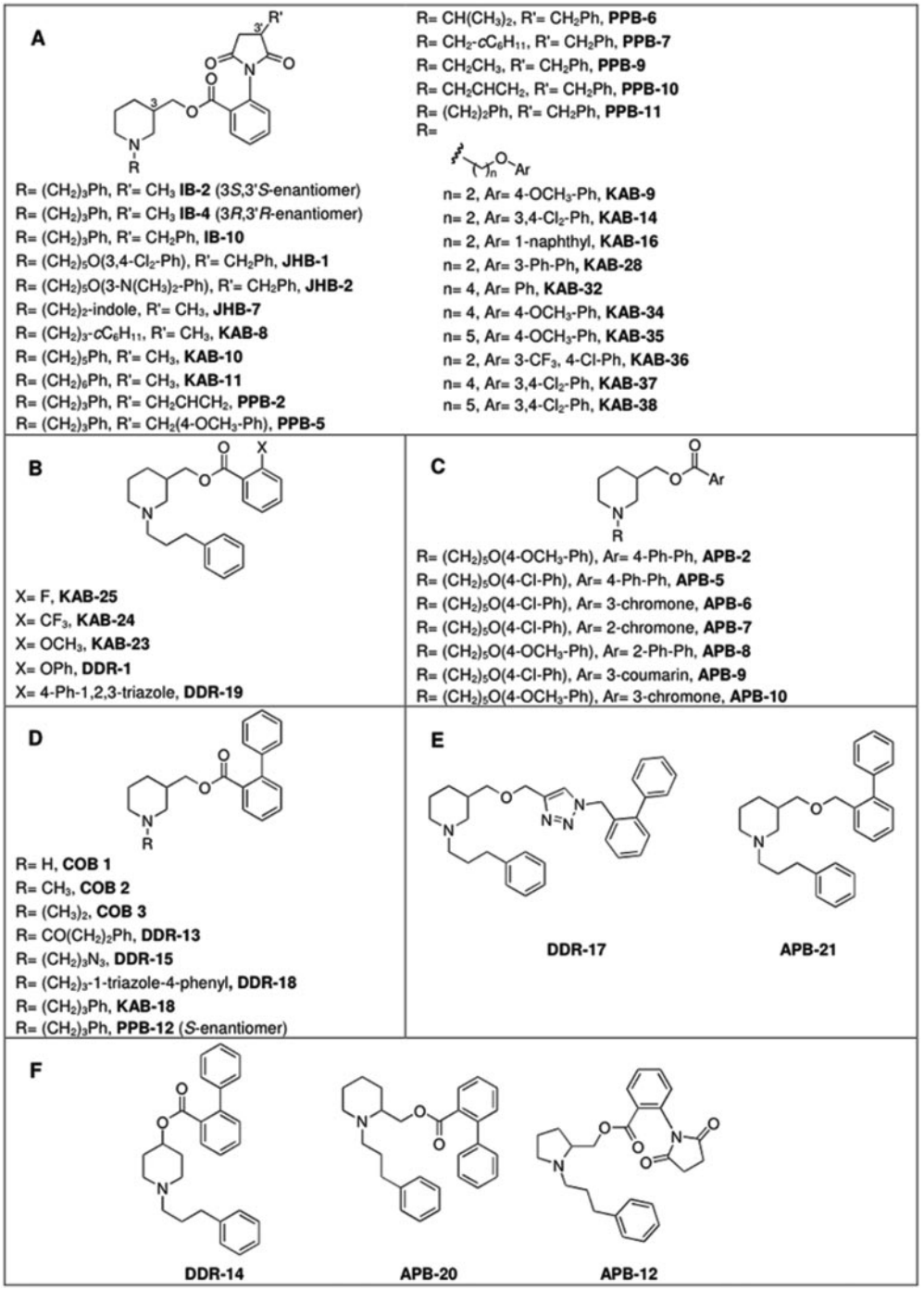

Fig. 1. Chemical structures.

ize the activity of drugs to nAChRs (e.g., McKay and Schneider, 1984). Inhibition of KCl-simulated neurosecretion will document additional inhibitory actions by the molecules (i.e., nonreceptor mechanisms). As seen in Fig. 6, the effects of the drugs at 10 μM concentrations varied from little (<25%) or no inhibitory activity to significant (>75%) inhibitory activity. These observations suggested that most of these drugs tested have at least two inhibitory effects: one effect mediated through nAChR mechanisms (seen with the calcium accumulation assays) and one effect mediated through non-nAChR mechanisms (seen with the KCl-neurosecretion assay). These data also suggested that the lack of correlation observed in Fig. 5 was due to these dual inhibitory activities. In support of this, a significant correlation using molecules with little or no non-nAChR effects was found when we directly compared IC_{50} values obtained from the nAChR-neurosecretion assays and the calcium accumulation assays ($r = 0.93$, $p < 0.0001$) (Fig. 7A). For drugs with large non-nAChR effects, no significant correlation was observed ($r = 0.36$, $p = 0.31$) (Fig. 7B).

In the next series of experiments, radiolabeled agonist binding studies were performed to investigate direct interactions of our molecules with the orthosteric site (i.e., competitive inhibition). The drugs (10 μM) showed little (<25%) or no inhibitory effects on [^{3}H]epibatidine binding to recombinant α3β4 nAChRs (Table 1). The effects of these drugs on

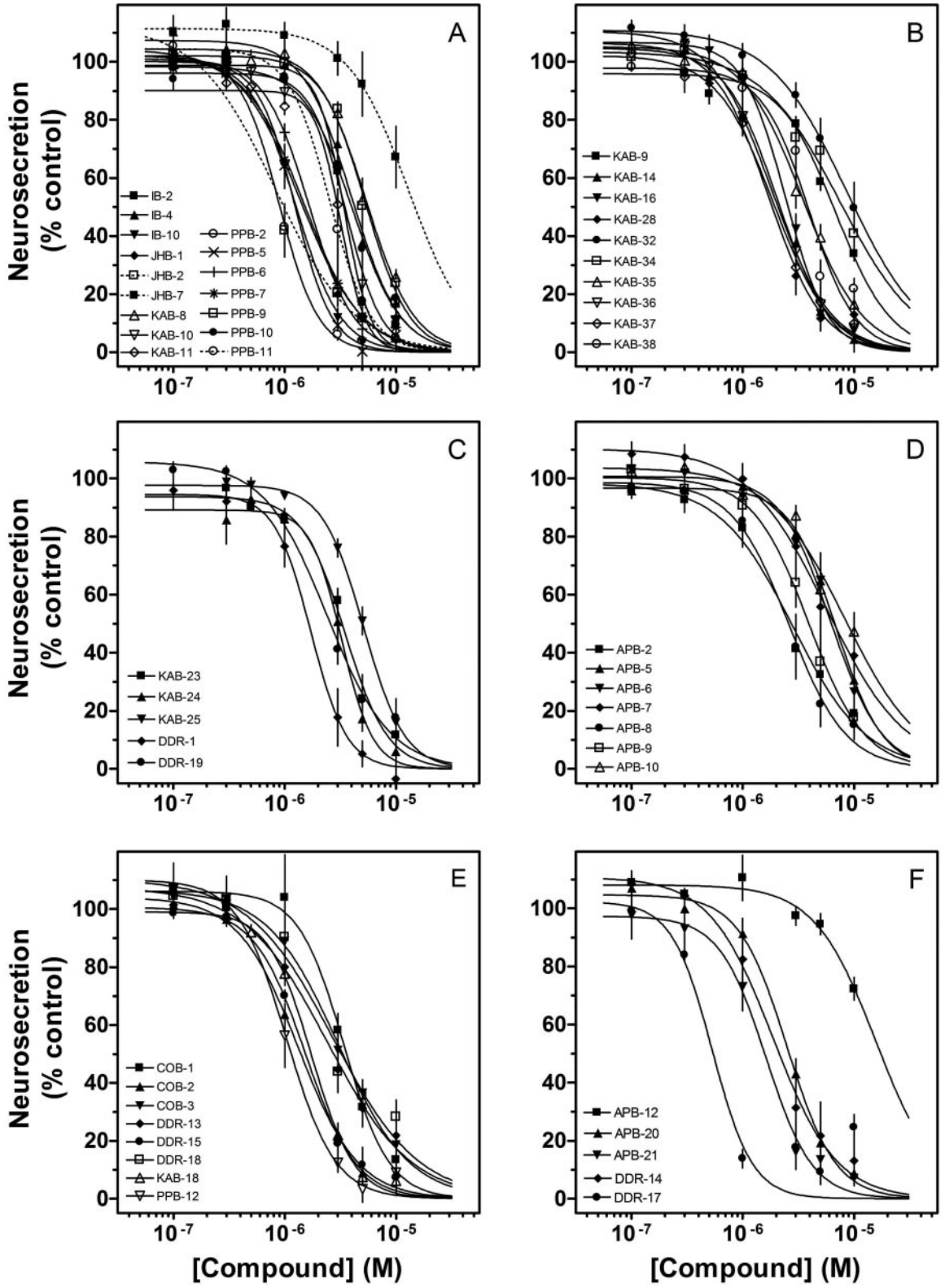

Fig. 2. Effects of drugs on adrenal neurosecretion stimulated via activation of native nAChRs. Cultured bovine adrenal chromaffin cells expressing α3β4* nAChRs were treated for 15 min with the drug before their stimulation with 10 μM nicotine in the continued presence of the drug. Concentration-response curves shown in A and B correspond to group A in Fig. 1. The concentration-response curves in C, D, and E correspond to groups B, C, and D, respectively. The concentration-response curves in F correspond to groups E and F. Values represent means ± S.E.M. (n = 3–8). Results are expressed as a percentage of control, nicotine-stimulated neurosecretion.

binding to native α3β4* nAChRs were somewhat more diverse than their effects on recombinant nAChRs, ranging from little (<20%) or no effects to large increases in binding (Table 1). At a concentration of 10 μM, approximately half (24/51) of our drugs increased (≥1.2-fold) [^{3}H]epibatidine binding; 16 of these molecules increased binding by 1.4- to

TABLE 1
Functional and binding effects of the nAChR negative allosteric modulators

Drug	Functional Studies				Binding Studies (nAChR Specific Binding[a,d])	
	Native nAChRs (Nicotine-Stimulated Neurosecretion)		Recombinant nAChRs (Nicotine-Stimulated $[Ca^{2+}]_i$)			
	IC_{50}[c]	n_H[d]	IC_{50}[c]	n_H[d]	Native nAChRs	Recombinant nAChRs
	μM		*μM*		*% Control*	
APB-2	2.8 (2.5–3.1)[e]	−1.3 ± 0.2	15.7 (11.9–20.8)[b]	−2.1 ± 1.1	118.6 ± 14.6	75.6 ± 9.6
APB-5	7.1 (5.8–8.7)[e]	−2.8 ± 1.0	38.2 (13.1–111.8)[b]	−1.1 ± 0.9	108.2 ± 11.2	75.5 ± 6.1
APB-6	6.6 (6.1–7.2)[e]	−2.1 ± 0.5	3.7 (3.5–3.8)	−1.3 ± 0.1	95.5 ± 8.1	98.5 ± 2.4
APB-7	6.7 (4.4–10.4)	−1.7 ± 0.3	3.8 (3.2–4.4)	−1.1 ± 0.1	103.4 ± 8.1	100.7 ± 2.7
APB-8	2.8 (2.1–3.9)[e]	−2.1 ± 0.2	10.0 (9.5–10.6)	−1.4 ± 0.5	174.4 ± 14.8	71.2 ± 3.9
APB-9	4.0 (3.2–4.8)[e]	−2.3 ± 0.4	4.2 (3.9–4.5)	−1.1 ± 0.1	107.3 ± 7.7	96.9 ± 1.6
APB-10	8.2 (6.9–9.8)[e]	−1.4 ± 0.2	2.6 (2.3–3.0)	−0.9 ± 0.0	98.7 ± 4.7	99.8 ± 1.8
APB-12	13.0 (10.8–16)[e]	−1.6 ± 0.2	6.6 (6.0–7.2)	−1.1 ± 0.2	98.7 ± 4.4	120.7 ± 9.3
APB-20	2.4 (2.3–2.6)	−2.1 ± 0.2	10.9 (9.1–13.2)[b]	−1.3 ± 0.4	112.8 ± 17.7	75.0 ± 5.8
APB-21	1.6 (1.3–1.9)	−3.2 ± 1.2	19.0 (12.8–28.3)[b]	−1.3 ± 0.6	130.3 ± 17.4	80.6 ± 3.4
COB-1	3.5 (3.1–3.9)[e]	−2.8 ± 1.3	1.2 (1.0–1.4)[e]	−0.7 ± 0.1	113.5 ± 4.8[e]	87.3 ± 2.6
COB-2	1.2 (1.2–1.3)[e]	−2.0 ± 0.2	1.1 (1.0–1.1)[e]	−0.8 ± 0.0	125.8 ± 3.8[e]	88.7 ± 1.5
COB-3	3.0 (2.5–3.7)[e]	−1.6 ± 0.5	0.7 (0.6–0.9)[e]	−0.9 ± 0.1	106.0 ± 2.5[e]	68.8 ± 5.6
DDR-1	1.7 (1.4–2.0)[e]	−5.1 ± 2.3	30.0 (23.5–38.3)[b,e]	−0.7 ± 0.1	118.7 ± 13.9[e]	66.3 ± 4.8
DDR-13	2.2 (1.8–2.7)	−1.3 ± 0.3	15.0 (12.1–18.3)[b]	−1.9 ± 0.7	224.3 ± 12.1	113.0 ± 7.3[g]
DDR-14	1.8 (1.4–2.1)	−1.7 ± 0.5	20.3 (13.4–30.6)[b]	−1.5 ± 0.7	216.6 ± 6.0	92.8 ± 6.1[g]
DDR-15	1.4 (1.3–1.5)	−2.6 ± 0.4	2.4 (2.2–2.6)	−0.9 ± 0.1	201.6 ± 6.3	103.1 ± 9.8[g]
DDR-17	0.4 (0.4–0.4)	−2.4 ± 0.5	7.7 (5.8–10.1)	−1.3 ± 0.3	215.0 ± 8.8	75.3 ± 8.1[g]
DDR 18	2.6 (2.3–3.0)	−1.2 ± 0.2	20.4 (14.1–29.6)[b]	−1.6 ± 0.6	190.6 ± 8.0	91.2 ± 10.1[g]
DDR-19	2.4 (2.2–2.6)	−1.7 ± 0.5	2.0 (1.5–2.7)	−1.0 ± 0.1	169.5 ± 5.6	91.6 ± 10.0[g]
IB-2	3.3 (3.2–3.3)	−3.9 ± 1.2	1.5 (1.3–1.9)	−1.1 ± 0.1	102.2 ± 6.5	78.4 ± 6.7
IB-4	3.5 (2.7–4.6)	−2.0 ± 0.2	4.8 (3.7–6.1)	−0.8 ± 0.1	107.0 ± 16.1	95.5 ± 7.5
IB-10	1.3 (1.1–1.4)[e]	−2.4 ± 0.3	7.6 (6.8–8.6)[e]	−1.4 ± 0.1	151.3 ± 15.7[e]	96.7 ± 7.0
JHB-1	1.3 (1.1–1.5)[e]	−3.9 ± 1.5	4.5 (4.0–5.1)	−1.0 ± 0.2	102.0 ± 13.5	87.2 ± 5.8
JHB-2	0.7 (0.6–0.8)	−3.9 ± 1.2	4.6 (4.1–5.2)	−0.7 ± 0.1	112.9 ± 12.2	100.1 ± 5.5
JHB-7	11.9 (9.7–14.6)	−4.0 ± 2.5	5.6 (5.2–6.0)	−1.3 ± 0.1	99.5 ± 3.6	74.3 ± 4.6
KAB-8	5.4 (5.0–5.8)[e]	−2.1 ± 0.2	5.2 (4.8–5.6)	−1.6 ± 0.1	137.4 ± 2.8	98.0 ± 3.8
KAB-9	6.9 (6.5–7.3)[e]	−1.8 ± 0.2	2.8 (2.5–3.1)	−0.9 ± 0.2	115.2 ± 3.0	95.1 ± 1.8
KAB-10	3.5 (3.5–3.6)[e]	−4.1 ± 0.5	4.5 (3.9–5.3)	−1.0 ± 0.1	146.9 ± 1.9	92.6 ± 4.4
KAB-11	2.8 (2.4–3.1)[e]	−4.2 ± 0.6	7.2 (6.3–8.3)	−1.4 ± 0.2	136.7 ± 16.9	89.1 ± 1.6
KAB-14	2.1 (1.9–2.4)[e]	−1.9 ± 0.2	6.8 (5.8–7.9)	−1.1 ± 0.3	111.8 ± 6.0	79.8 ± 6.9
KAB-16	2.5 (2.2–2.8)[e]	−2.3 ± 0.1	6.1 (5.1–7.3)	−1.2 ± 0.2	108.4 ± 3.4	82.8 ± 4.2
KAB-18	1.7 (1.6–1.8)[e]	−2.2 ± 0.1	10.2 (7.9–13.3)	−1.1 ± 0.2	110.1 ± 14.1	69.9 ± 3.8
KAB-23	3.2 (3.1–3.4)[f]	−2.3 ± 0.1	1.9 (1.7–2.1)	−0.8 ± 0.1	135.3 ± 12.8	77.6 ± 2.6
KAB-24	3.2 (3.1–3.2)[f]	−1.9 ± 0.3	2.7 (2.2–3.3)	−0.7 ± 0.1	173.5 ± 16.1	72.1 ± 1.8
KAB-25	5.2 (4.8–5.6)[f]	−2.4 ± 0.2	2.6 (2.2–3.1)	−1.2 ± 0.0	145.2 ± 11.4	70.1 ± 3.7
KAB-28	1.8 (1.6–2.1)	−1.9 ± 0.4	12.2 (10.4–14.4)[b]	−1.5 ± 0.5	127.5 ± 4.7	71.8 ± 3.7
KAB-32	6.7 (6.0–7.5)	−1.7 ± 0.6	1.6 (1.4–1.9)	−1.1 ± 0.1	97.9 ± 7.9	108.6 ± 15.5
KAB-34	6.2 (5.3–7.2)[e]	−1.6 ± 0.7	3.1 (2.8–3.5)[e]	−1.1 ± 0.1	83.2 ± 1.4[e]	79.9 ± 11.4
KAB-35	3.3 (2.8–3.9)[e]	−1.7 ± 0.3	6.2 (5.6–6.8)	−1.4 ± 0.1	68.7 ± 3.7	71.0 ± 29.1[g]
KAB-36	2.0 (1.8–2.2)[e]	−1.9 ± 0.1	20.3 (19.4–21.2)[b]	−1.0 ± 0.3	121.6 ± 11.5	95.6 ± 28.1
KAB-37	1.9 (1.6–2.2)[e]	−1.8 ± 0.2	9.5 (9.1–9.8)	−1.2 ± 0.2	138.9 ± 5.3	92.1 ± 7.0
KAB-38	3.5 (3.2–3.8)[e]	−4.4 ± 1.9	11.9 (10.8–13.2)[b]	−1.4 ± 0.7	139.9 ± 6.0	93.5 ± 10.4
PPB-2	0.9 (0.8–1.0)	−3.2 ± 0.1	17.2 (12.4–23.9)[b]	−0.6 ± 0.3	147.7 ± 7.7	97.9 ± 2.6
PPB-5	1.2 (1.1–1.3)[e]	−2.7 ± 0.5	13.4 (10.3–17.3)[b,e]	−0.7 ± 0.3	152.8 ± 7.6[e]	90.3 ± 1.1
PPB-6	1.6 (1.6–1.7)[e]	−2.4 ± 0.3	1.8 (1.5–2.0)	−0.6 ± 0.1	123.8 ± 7.6	101.8 ± 1.5
PPB-7	1.2 (1.1–1.3)[e]	−4.1 ± 2.2	4.6 (4.0–5.3)	−1.0 ± 0.1	144.3 ± 9.4	89.1 ± 3.7
PPB-9	5.7 (5.0–6.5)[e]	−2.9 ± 0.4	3.1 (2.3–4.2)	−0.7 ± 0.1	112.7 ± 2.1	96.6 ± 5.1
PPB-10	4.1 (3.8–4.5)[e]	−3.8 ± 1.1	2.6 (2.1–3.2)	−1.0 ± 0.1	118.8 ± 4.4	92.7 ± 3.2
PPB-11	2.6 (2.2–3.1)[e]	−2.9 ± 0.4	8.0 (5.9–10.8)[e]	−1.3 ± 0.4	118.4 ± 12.5[e]	104.0 ± 16.4
PPB-12	1.1 (0.9–1.3)	−3.6 ± 1.2	21.0 (15.4–28.4)[b]	−0.8 ± 0.3	117.9 ± 6.7	83.3 ± 16.1

n_H, Hill coefficient.
[a] The effects of the analogs were determined at a fixed concentration of 10 μM.
[b] Extrapolated IC_{50} values taken from mean curves.
[c] Values represent geometric means (confidence limits), $n = 3$ to 8.
[d] Values represent arithmetic means ± S.E.M. ($n = 3$–12).
[e] Values from McKay et al. (2007).
[f] Values from Bergmeier et al. (2004).
[g] Values represent means ± S.D. ($n = 2$).

2.3-fold (Table 1). The concentration dependencies of the binding effects for several molecules are seen in Fig. 8. When homologous competition binding experiments were performed in the absence or presence of 10 μM APB-8, the IC_{50} values of epibatidine significantly ($p < 0.01$) decreased from 1.51 (1.45–1.58) nM in the absence to 0.97 (0.90–1.05) nM in the presence of APB-8 (Fig. 9). APB-8 also increased total [^{3}H]epibatidine binding (Fig. 9, inset), but it did not affect nonspecific binding (data not shown). The data suggested that the observed increase in radiolabeled ligand binding in the presence of the drugs was at least partially due to an increase in apparent affinity of the radiolabeled ligand for its binding site.

In this final series of experiments, computational homology modeling and blind docking approaches were used to identify the potential binding site of our negative allosteric

TABLE 2
Comparison of effects of agonists and antagonists on functional responses from native and recombinant α3β4 nAChRs

	Recombinant Rat α3β4 nAChRs[a] ($[Ca^{2+}]_i$) EC_{50} or IC_{50}	Native Bovine α3β4* nAChRs (Neurosecretion) EC_{50} or IC_{50}
	μM	
Nicotine	18.0 (15.9–20.4)	3.6 (2.9–4.5)[b]
Epibatidine	0.06 (0.05–0.07)	0.009 (0.006–0.014)[b]
d-Tubocurarine	6.3 (5.0–8.1)	2.2 (1.4–3.6)[c]
Mecamylamine	0.6 (0.4–0.8)	0.1 (0.1–0.7)[d]
Tetracaine	2.5 (2.4–2.6)	4.0 (2.2–7.4)[d]
COB-2	1.1 (1.0–1.1)[e]	1.2 (1.2–1.3)[e]

[a] Data are means (confidence limits) of three to four different experiments performed in triplicate or quadruplicate.
[b] EC_{50} value from Wenger et al. (1997).
[c] IC_{50} value from McKay and Burkman (1993).
[d] IC_{50} value from McKay and Trent-Sanchez (1990).
[e] IC_{50} value from McKay et al. (2007) and Table 1.

modulators. We hypothesized that since these molecules are structurally similar to MLA (Bergmeier et al., 1999, 2004; Bryant et al., 2002; McKay et al., 2007) and MLA is a competitive antagonist for α3β4 nAChRs (Free et al., 2003), the binding site of the negative allosteric modulators would be near the orthosteric binding site. Two stereoisomers of COB-3 were docked to 72 receptor conformations taken at 200-ps intervals over the duration of an MD simulation of the agonist-bound model. COB-3 was chosen because of its relatively high potency. The most frequently occurring docking cluster for COB-3 is shown in Fig. 10. This position on the receptor was the consensus docking site for both COB-3 stereoisomers. After docking to receptor conformations that represent 15 ns of simulation, one of the top four docking clusters for the two COB-3 compounds occurred at the most prominent site in 58.3% of the receptor conformations that were docked to, whereas the second most prominent site had an occurrence rate of 42.4%. The site characterized in Fig. 10 was located within the pore of an α/β interface, ~7 Å from the bound epibatidine in the agonist binding site. This docking site remained the most prominent site over the duration of the simulation (20 and 72 snapshots), supporting consistency of the data and lack of stereoselectivity at the site. Key interactions included a hydrogen bonding potential between the ester linkage of COB-3 with Asn108 and a stabilizing electrostatic interaction between the positively piperidine moiety of the ligand and Asp88. All stereoisomers of three additional compounds (PPB-9, APB-10, and APB-12), representative of the various chemical scaffolds (Fig. 1), were also blind-docked to the homology models in an identical manner as described for COB-3; all of these compounds were docked to the same corresponding site (data not shown).

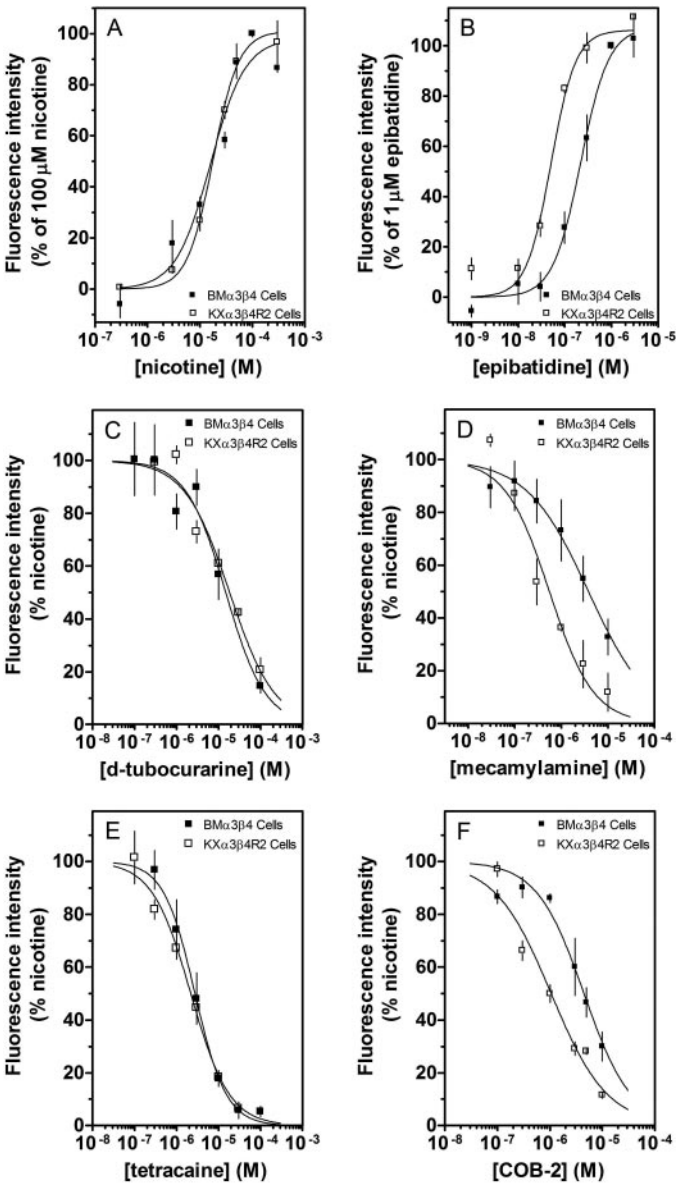

Fig. 3. Comparison of effects of agonists and antagonists on HEK 293 cells expressing either rat or bovine recombinant nAChRs. KXα3β4R2 (□) and BMα3β4 (■) cells were loaded with fluo-4-AM for 60 min. For BMα3β4 cells, experiments were performed in buffer containing 20 mM calcium. Fluorescence was measured after stimulation with increasing concentrations of nicotine (A) or epibatidine (B). Effects of *d*-tubocurarine (C), mecamylamine (D), tetracaine (E), and COB-2 (F) on nicotine (100 μM)-stimulated increases in calcium accumulation were also determined. Results are expressed as either the percentage of the effect of 100 μM nicotine (A), the percentage of the effect of 1 μM epibatidine (B), or the percentage of control, nicotine-stimulated peak fluorescence levels (C–F). Values represent means ± S.E.M. (n = 3–4).

Discussion

Our laboratory has identified a series of molecules that inhibit nAChR-mediated neurosecretion (Bergmeier et al., 1999, 2004; Bryant et al., 2002; McKay et al., 2007). In the studies reported here using cells expressing recombinant nAChRs, we confirm that these drugs act at the level of the nAChR to noncompetitively inhibit activation of nAChRs. The calcium accumulation assay is directly linked to nAChR activation (Stauderman et al., 1998; Chavez-Noriega et al., 2000). The IC_{50} values of our molecules ranged from 0.7 to 38.2 μM. Their potencies are similar to other inhibitors of adrenal neurosecretion, including *d*-tubocurarine, hexamethonium, decamethonium, tetracaine, pentolinium, and mecamylamine (IC_{50} values ranging from 17 to 0.1 μM) (McKay and Trent-Sanchez, 1990; McKay and Burkman, 1993).

Our compounds (51/51) showed an average increase in agonist binding of 1.3-fold, with approximately 50% (24/51) of these drugs (10 μM) increasing [^{3}H]epibatidine binding to the orthosteric site by an average of 1.6-fold. This drug-induced increase in binding to the agonist binding site is at least partially due to an increase in affinity of epibatidine to this site (Fig. 9). Many noncompetitive antagonists have

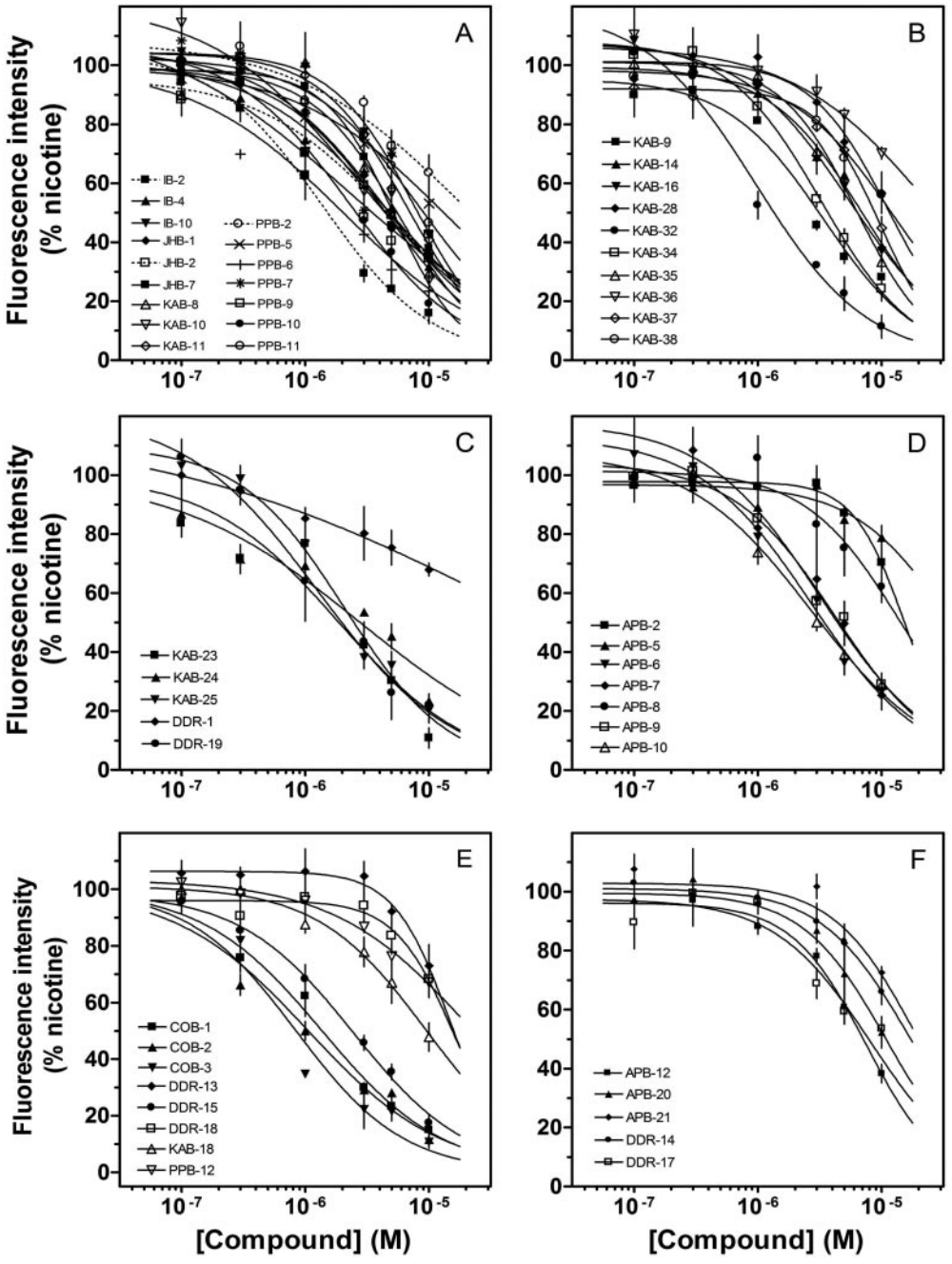

Fig. 4. Effects of drugs on intracellular calcium levels stimulated via activation of recombinant nAChRs. Cultured KXα3β4R2 cells were loaded with fluo-4-AM for 60 min and treated with the drug 40 s before their stimulation with 100 μM nicotine in the continued presence of the drug. Concentration-response curves shown in A and B correspond to group A in Fig. 1. The concentration-response curves in C to E correspond to groups B, C, and D, respectively. The concentration-response curves in F correspond to groups E and F. Values represent means $\pm$ S.E.M. (n = 3–4). Results are expressed as percentage of control, nicotine-stimulated peak fluorescence levels.

shown to enhance agonist binding to the AChR orthosteric site (Kato and Changeux, 1976; Herz et al., 1987), including NAMs (Herz et al., 1987), and these increases in agonist binding to the orthosteric site have been linked to desensitization of nAChRs (Kato and Changeux, 1976). In addition, similar increases in agonist binding affinity have been reported for noncompetitive antagonists; chlorpromazine and vinblastine decrease IC_{50} values from 4.3 to 1.6 μM (Carp et al., 1983) and from ~0.5 to 0.1 μM (McKay et al., 1985), respectively, and dibucaine and histrionicotoxin decreased IC_{50} values from 20.7 to 8.6 μM and 21.0 to 2.6 μM, respectively (Sine and Taylor, 1982). The binding of NAMs to allosteric sites may shift the receptors from the resting to the desensitized state or may stabilize the desensitized state; in either case, these desensitized receptors are not functional (Monod et al., 1965; Quick and Lester, 2002). The ability of our molecules to increase agonist binding to orthosteric sites of native nAChRs supports their classification as NAMs and suggests that their inhibitory actions involve receptor desensitization. No increases in agonist binding to recombinant receptors were observed, though. The reasons for these findings are unknown but may be due to potential differences in the subunit composition of native and recombinant α3β4 nAChRs; it has been reported that native α3β4* nAChRs may contain α5 or α7 subunits (Campos-Caro et al., 1997; Gerzanich et al., 1998; El-Hajj et al., 2007).

The data indicate that many of our allosteric modulators have additional, non-nAChR inhibitory activity. From a drug development perspective, it is important to identify drugs that have non-nAChR activity to reduce potentially problem-

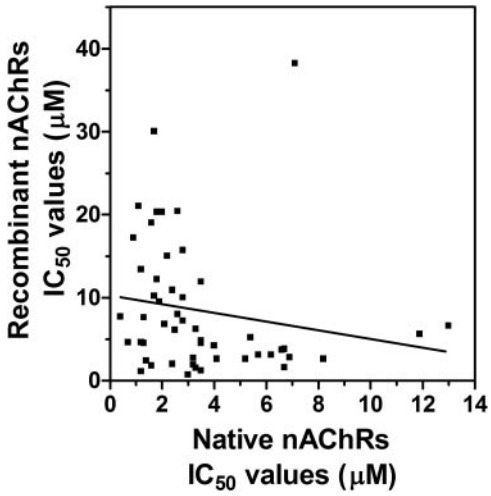

Fig. 5. Comparison of effects of drugs on recombinant and native nAChRs. Linear regression analysis of IC_{50} values of all our drugs on nicotine-stimulated calcium accumulation (recombinant nAChRs) and adrenal neurosecretion (native nAChRs) was performed. Actual IC_{50} values for recombinant nAChRs are found in Table 1. Values for native nAChRs are from McKay et al. (2007) and Bergmeier et al. (2004).

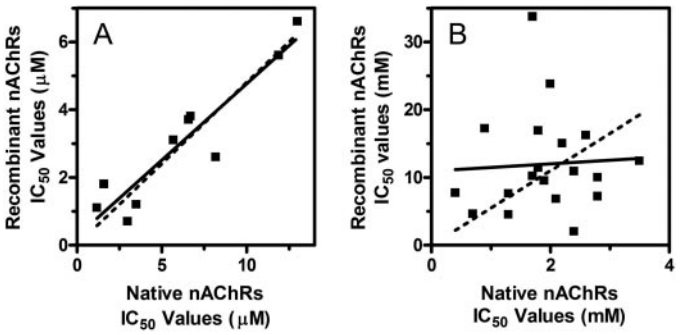

Fig. 7. Regression analyses comparing the effects of antagonists on recombinant and native nAChRs. Linear regression analysis of IC_{50} values obtained using nAChR antagonists with little or no non-nAChR effects (A: COB-3, APB-10, APB-6, APB-12, COB-1, PPB-9, APB-7, JHB-7, PPB-6, and COB-2) or nAChR antagonists with large non-nAChR actions (B: KAB-28, KAB-14, DDR-18, JHB-2, IB-10, DDR-1, DDR-17, KAB-38, JHB-1, and KAB-18) on nicotine-stimulated increase in intracellular calcium (recombinant nAChRs) and adrenal neurosecretion (native nAChRs). Actual IC_{50} values are found in Table 1. Dotted lines represent linear regression analyses when the data are forced through $x = 0, y = 0$.

atic side effects. Comparisons of Hill coefficients of inhibition curves in the two functional assays (native versus recombinant nAChRs) support differences in mechanisms of inhibition of the antagonists. The Hill coefficients of antagonists in the neurosecretion assay have a mean value of -2.53 ± 0.13, suggesting positive cooperativity. In contrast, the Hill coefficients of the antagonists in the calcium accumulation assay have a mean value of -1.11 ± 0.05, suggesting lack of cooperativity. These results indicate that the inhibitory mechanisms of the antagonists in the calcium accumulation assay probably involve a single site of action. In addition, approx-

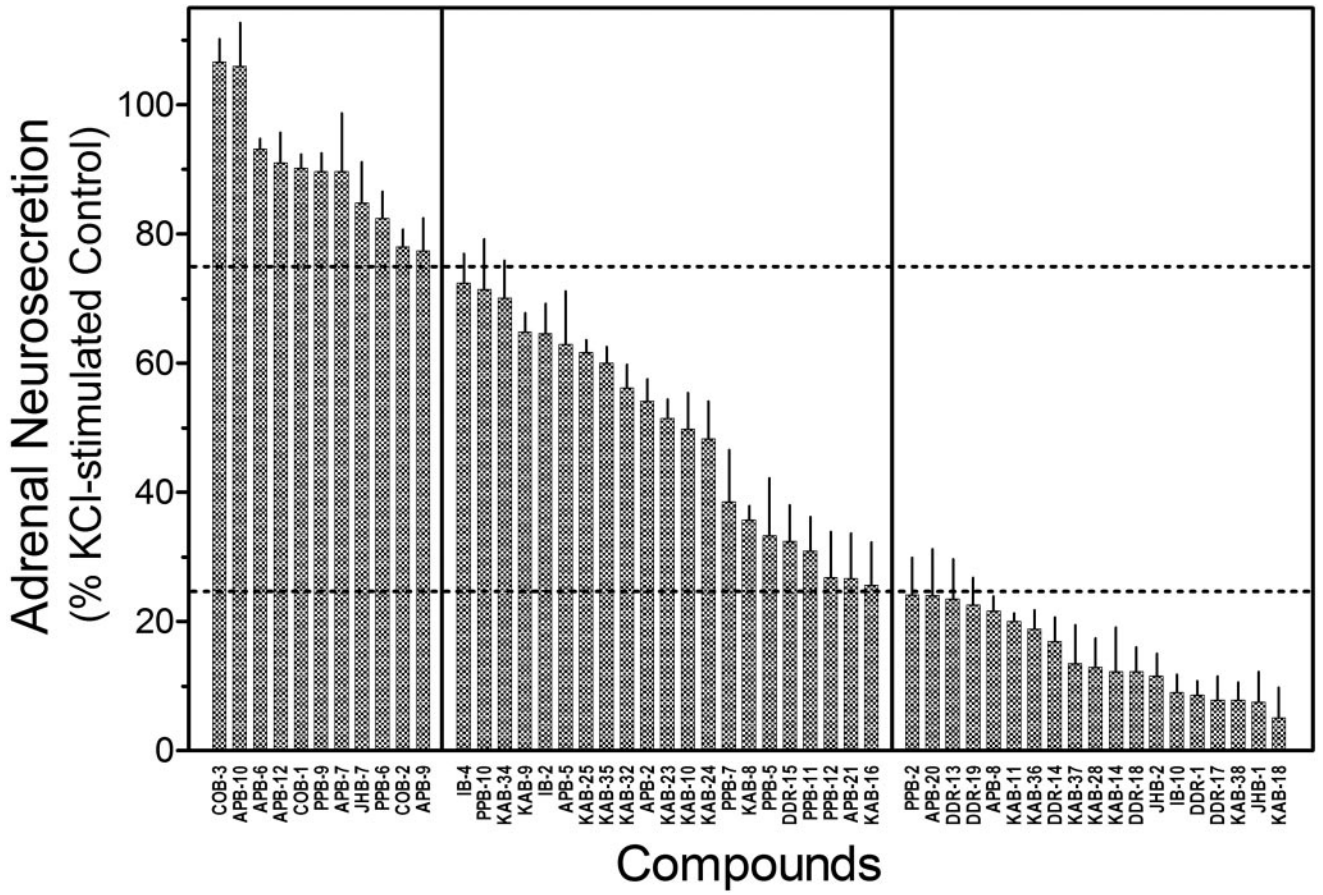

Fig. 6. Effects of nAChR Antagonists on KCl-stimulated Neurosecretion. KCl-stimulated neurosecretion studies were performed, as described under *Materials and Methods*, using a single concentration (10 μM) of each compound. Results are expressed as percentage of control, KCl-stimulated neurosecretion. Values represent means ± S.E.M. ($n = 4$–9).

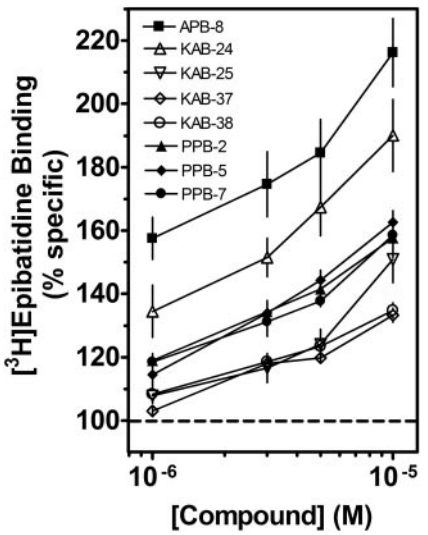

Fig. 8. Effects of nAChR antagonists on [^{3}H]epibatidine binding to native nAChRs. Competition binding experiments were performed on bovine adrenal medulla membrane homogenates using indicated concentrations of the molecules. Data are expressed as a percentage of control specific binding. Values represent means ± S.E.M. (n = 4).

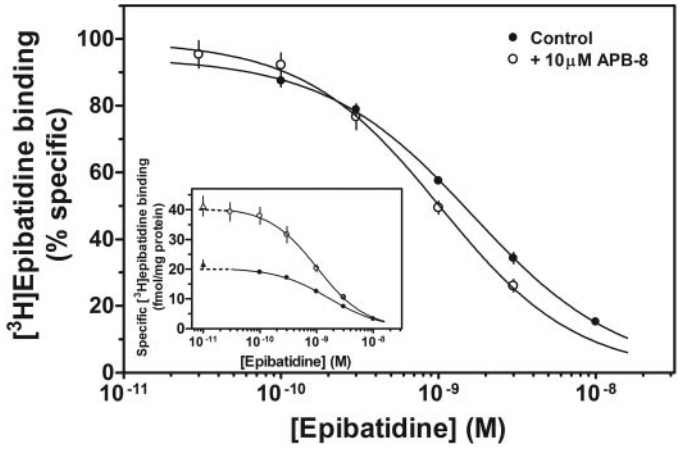

Fig. 9. Effects of APB-8 on [^{3}H]epibatidine binding. [^{3}H]epibatidine homologous competition binding experiments were performed on adrenal medulla membranes in the absence (●) and presence of 10 μM APB-8 (○). Data are expressed as percentage specific [^{3}H]epibatidine binding or as specific [^{3}H]epibatidine binding in femtomoles per milligram of protein (inset). Triangles represent [^{3}H]epibatidine binding in the absence of epibatidine (inset). Values represent means ± S.E.M. (n = 4).

imately 80% of our molecules (40/51) inhibit KCl-stimulated neurosecretion by 25% and more, establishing that these drugs interact with steps in the stimulus-secretion process distal to membrane depolarization (i.e., nonreceptor mechanisms). The KCl-neurosecretion assay was found to be a useful secondary assay for the screening of NAMs for additional, non-nAChR inhibitory activity. The correlation data in Fig. 7 support this approach. Drugs that inhibit neurosecretion stimulated via direct depolarization of cells must act on a site distal to nAChR activation. Additional sites of action may include other cationic channels (Na^+, K^+, and/or Ca^{2+} channels). Several drugs have been identified that target both nAChRs and ion channels. Galantamine, an nAChR allosteric potentiator, blocks K^+ channels in chromaffin cells (Alés et al., 2006) and hippocampal neurons (Pan et al., 2003). Nicardipine and other dihydropyridines, which are voltage-gated calcium channel blockers, inhibit nAChR activation in rat superior cervical ganglion neurons (Wheeler et al., 2006), in skeletal muscle (Adam and Henderson, 1990), and adrenal chromaffin cells (López et al., 1993).

Analyses of the structure-activity relationship studies were performed to investigate structural determinants of our drugs that affect their interactions with nAChR and non-nAChR sites. We focused on both potency of our drugs, obtained from their direct actions on nAChRs (calcium accumulation), and their non-nAChR related actions (KCl-mediated neurosecretion). The general structure of most compounds is that of a piperidine ring linked to a substituted benzoyl group via a hydroxymethyl group on the piperidine ring. One of the most drastic and important findings is that the replacement of the phenylpropyl group in KAB-18 [IC_{50} value = 10.2 (7.9–13.3) μM and >90% non-nAChR actions] with a small group both increases potency and eliminates non-nAChR-related effects. For example, COB-3 showed a 14-fold increase in potency and an elimination of non-nAChR-related actions. Similar differences were found with COB-1 and COB-2. Clearly, small alkyl groups on the piperidine nitrogen can provide potent drugs when coupled with the biphenyl ester. However, the biphenyl ester is not sufficient to enhance potency of large alkyl groups on the piperidine nitrogen (e.g., DDR-18). In addition to these biphenyl esters, compounds PPB-6 and PPB-9 provide similar pharmacological enhancements. Both of these compounds have a small alkyl group (*N*-iPr for PPB-6 and *N*-Et for PPB-9) on the piperidine nitrogen. Unlike compounds COB-1, -2, and -3, these compounds have a benzyl-substituted succinimide on the benzoyl group. This combination of a relatively large benzoyl group (biphenyl or benzyl-substituted succinimide) and a small alkyl group on the piperidine provide an interesting divergence from observations reported previously by our laboratory (Bryant et al., 2002). We should note that the replacement of the small alkyl group of PPB-6 with the larger 3-phenylpropyl group (IB-10) provides compounds essentially similar in both potency and non-nAChR-related effects to KAB-18.

Another structural set of compounds that have improved pharmacological properties are those exemplified by ABP-6, APB-7, APB-9, and APB-10. This set of compounds showed improved potency (~3–4-fold) and an elimination of non-nAChR-related actions. Structurally, these compounds contain a large alkyl group on the piperidine nitrogen. Unlike all of the other compounds examined, the benzoyl group has been replaced with a heterocyclic group (a chromone or coumarin). It is interesting to note that both 2- and 3-substituted chromones have roughly similar activities. In addition, substitution on the terminal end of the piperidine alkyl substituent (4-methoxyphenyl in APB-10 compared with the 4-chlorophenyl of APB-6) again showed only minor differences. A final compound that showed improved pharmacological properties is APB-12. This compound is almost identical to IB-2; the only difference is the change of the piperidine ring of IB-2 to a pyrrolidine ring and a change in the position of the hydroxymethyl linker to the benzoyl group.

The structure-activity relationship studies reported here have allowed us identify three general structural classes of molecules with improved pharmacological profiles relative to initially identified compounds. One group has a small alkyl group on the piperidine nitrogen and a large benzoyl ester. The other group has a large alkyl group on the piperidine nitrogen and a heterocyclic ester. The final group of one

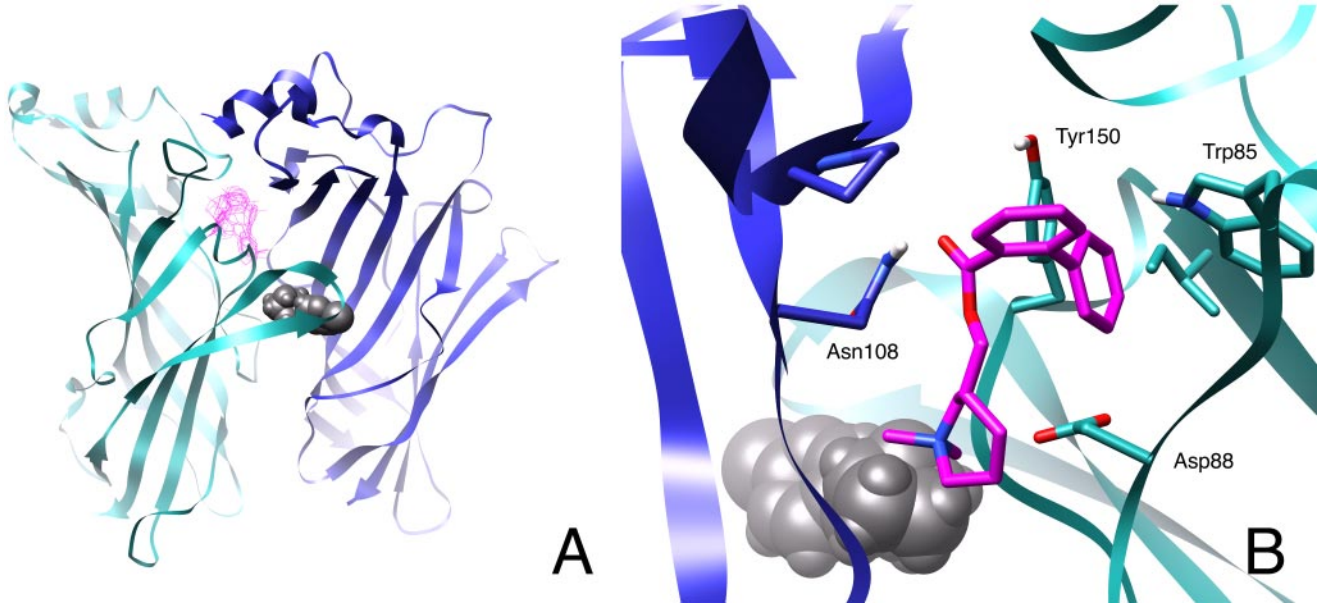

Fig. 10. Docking of COB-3 to a computational model of the α3β4 nAChR. A, position of the most frequent COB-3 (pink) docking cluster on the rat α3β4 nAChR LBD model. The docking position is at the α/β interface on the pore-side of the channel. Three of the five subunits are not shown for clarity. B, detailed interactions of COB-3 at the α/β interface as viewed from inside the pore. The α3 subunit is shown in cyan and the β4 subunit is in blue. Epibatidine is shown in gray at the agonist binding site.

contains both a large piperidine alkyl substituent and a large benzoyl group on a pyrrolidine ring. Molecules that fall outside these general structural requirements while potent tend to exhibit significant non-nAChR activity.

Using homology modeling and blind docking approaches, we identified a potential binding site for our NAMs, ~7 Å from the agonist binding site. This binding site, as we hypothesized, is adjacent to the binding site of MLA (Hansen et al., 2005). Interestingly, the docking site identified for COB-3 is similar in position to that of the nAChR allosteric potentiator galantamine, which was also identified via blind docking (Iorga et al., 2006).

In summary, we have shown that our primary assay (calcium accumulation) and our secondary assay (KCl-neurosecretion) are important in nAChR drug development. We have identified several molecules showing promise as NAMs of nAChRs. Although our paradigms involve either native or recombinant α3β4 nAChRs, these drugs show limited nAChR subtype selectivity (data not shown); however, computer-assisted drug design is currently being investigated to improve selectivity. To date, we have discovered a small group of drugs that 1) inhibit adrenal nAChR-activated neurosecretion, 2) inhibit nAChR-activated increases in intracellular calcium from cells expressing recombinant nAChRs, 3) exert little or no effects on non-nAChR-mediated neurosecretion, and 4) exert little or no inhibitory effects on binding to native and recombinant adrenal nAChRs. Correlation of functional data (Fig. 7A) supports a single site of action of this group of drugs on nAChRs. The structure-activity relationship study emphasizes that small substitutions to the piperidine ring or to the benzoyl ester also improve potency and avoid non-nAChR actions. Computational modeling and blind docking identify a binding site for our NAMs near the orthosteric binding site of the receptor. The localization and characterization of the binding site for these novel drugs should provide insight into synthetic alterations that will produce more potent and more selective antagonists for specific subtypes of nAChRs. The discovery of novel nAChR negative allosteric modulators will provide new experimental approaches to investigate nAChR involvement in physiological functions and pathophysiological conditions and, possibly, novel therapeutic strategies to treat disease.

Acknowledgments

The KXα3β4R2 cells were kindly provided by Drs. Xiao and Kellar (Georgetown University). We thank the Ohio Supercomputer Center for a grant of computational resources.

References

Adam LP and Henderson EG (1990) Calcium channel effectors are potent non-competitive blockers of acetylcholine receptors. *Pflugers Arch* **416:**586–593.

Alés E, Gullo F, Arias E, Olivares R, García AG, Wanke E, and López MG (2006) Blockade of Ca^{2+}-activated K^+ channels by galantamine can also contribute to the potentiation of catecholamine secretion from chromaffin cells. *Eur J Pharmacol* **548:**45–52.

Arias HR, Bhumireddy P, and Bouzat C (2006) Molecular mechanisms and binding site locations for noncompetitive antagonists of nicotinic acetylcholine receptors. *Int J Biochem Cell Biol* **38:**1254–1276.

Bergmeier SC, Ismail KA, Arason KM, McKay S, Bryant DL, and McKay DB (2004) Structure activity studies of ring E analogues of methyllycaconitine. Part 2: synthesis of antagonists to the α3β4 nicotinic acetylcholine receptors through modifications to the ester. *Bioorg Med Chem Lett* **14:**3739–3742.

Bergmeier SC, Lapinsky DJ, Free RB, and McKay DB (1999) Ring E analogs of methyllycaconitine (MLA) as novel nicotinic antagonists. *Bioorg Med Chem Lett* **9:**2263–2266.

Bryant DL, Free RB, Thomasy SM, Lapinsky DJ, Ismail KA, McKay SB, Bergmeier SC, and McKay DB (2002) Structure-activity studies with ring E analogues of methyllycaconitine on bovine adrenal α3β4* nicotinic receptors. *Neurosci Res* **42:**57–63.

Campos-Caro A, Smillie FI, Domínguez del Toro E, Rovira JC, Vicente-Agulló F, Chapuli J, Juíz JM, Sala S, Sala F, Ballesta JJ, et al. (1997) Neuronal nicotinic acetylcholine receptors on bovine chromaffin cells: cloning expression and genomic organization of receptor subunits. *J Neurochem* **68:**488–497.

Carp JS, Aronstam RS, Witkop B, and Albuquerque EX (1983) Electrophysiological and biochemical studies on enhancement of desensitization by phenothiazine neuroleptics. *Proc Natl Acad Sci U S A* **80:**310–314.

Cassels BK, Bermúdez I, Dajas F, Abin-Carriquiry JA, and Wonnacott S (2005) From ligand design to therapeutic efficacy: the challenge for nicotinic receptor research. *Drug Discov Today* **10:**1657–1665.

Celie PH, van Rossum-Fikkert SE, van Dijk WJ, Brejc K, Smit AB, and Sixma TK (2004) Nicotinic and carbamylcholine binding to nicotinic acetylcholine receptors as studied in AChBP crystal structures. *Neuron* **41:**907–914.

Celie PH, Klaassen RV, van Rossum-Fikkert SE, van Elk R, van Nierop P, Smit AB, and Sixma TK (2005) Crystal structure of acetylcholine-binding protein from *Bulinus truncatus* reveals the conserved structural scaffold and sites of variation in nicotinic acetylcholine receptors. *J Biol Chem* **280:**26457–26466.

Chavez-Noriega LE, Gillespie A, Stauderman KA, Crona JH, Claeps BO, Elliott KJ, Reid RT, Rao TS, Velicelebi G, Harpold MM, et al. (2000) Characterization of the recombinant human neuronal nicotinic acetylcholine receptors α3β2 and a4β2 stably expressed in HEK293 cells. *Neuropharmacology* **39:**2543–2560.
Costa V, Nistri A, Cavalli A, and Carloni P (2003) A structural model of agonist binding to the α3β4 neuronal nicotinic receptor. *Br J Pharmacol* **140:**921–931.
Dellisanti CD, Yao Y, Stroud JC, Wang ZZ, and Chen L (2007) Crystal structure of the extracellular domain of nAChR α1 bound to α-bungarotoxin at 1.94 Å resolution. *Nat Neurosci* **10:**953–962.
Dwoskin LP and Crooks PA (2001) Competitive neuronal nicotinic receptor antagonists: a new direction for drug discovery. *J Pharmacol Exp Ther* **298:**395–402.
El-Hajj RA, McKay SB, and McKay DB (2007) Pharmacological and immunological identification of native α7 nicotinic receptors: evidence for homomeric and heteromeric α7 receptors. *Life Sci* **81:**1317–1322.
Free RB, von Fischer ND, Boyd RT, and McKay DB (2003) Pharmacological characterization of recombinant bovine α3β4 neuronal nicotinic receptors stably expressed in HEK 293 cells. *Neurosci Lett* **343:**180–184.
Gerzanich V, Wang F, Kuryatov A, and Lindstrom J (1998) α5 Subunit alters desensitization, pharmacology, Ca^{++} permeability and Ca^{++} modulation of human neuronal α3 nicotinic receptors. *J Pharmacol Exp Ther* **286:**311–320.
Hansen SB, Sulzenbacher G, Huxford T, Marchot P, Taylor P, and Bourne Y (2005) Structures of *Aplysia* AChBP complexes with nicotinic agonists and antagonists reveal distinctive binding interfaces and conformations. *EMBO J* **24:**3635–3646.
Herz JM, Johnson DA, and Taylor P (1987) Interaction of noncompetitive inhibitors with the acetylcholine receptor. The site specificity and spectroscopic properties of ethidium binding. *J Biol Chem* **262:**7238–7247.
Huang J, Orac CM, McKay S, McKay DB, and Bergmeier SC (2008) The synthesis of 5-substituted ring E analogs of methyllycaconitine via the Suzuki-Miyaura cross-coupling reaction. *Bioorg Med Chem* **16:**3816–3824.
Iorga B, Herlem D, Barré E, and Guillou C (2006) Acetylcholine nicotinic receptors: finding the putative binding site of allosteric modulators using the "blind docking" approach. *J Mol Model* **12:**366–372.
Kato G and Changeux JP (1976) Studies on the effect of histrionicotoxin on the monocellular electroplax from *Electrophorus electricus* and on the binding of (^{3}H)acetylcholine to membrane fragments from *Torpedo marmorata. Mol Pharmacol* **12:**92–100.
Lin JH, Perryman AL, Schames JR, and McCammon JA (2003) The relaxed complex method: accommodating receptor flexibility for drug design with an improved scoring scheme. *Biopolymers* **68:**47–62.
Lloyd GK and Williams M (2000) Neuronal nicotinic acetylcholine receptors as novel drug targets. *J Pharmacol Exp Ther* **292:**461–467.
López MG, Fonteríz RI, Gandía L, de la Fuente M, Villarroya M, García-Sancho J, and García AG (1993) The nicotinic acetylcholine receptor of the bovine chromaffin cell, a new target for dihydropyridines. *Eur J Pharmacol* **247:**199–207.
McKay DB and Burkman AM (1993) Nicotinic and non-nicotinic receptor-mediated actions of vinblastine. *Proc Soc Exp Biol Med* **203:**372–376.
McKay DB and Schneider AS (1984) Selective inhibition of cholinergic receptor-mediated $^{45}Ca^{++}$ uptake and catecholamine secretion from adrenal chromaffin cells by taxol and vinblastine. *J Pharmacol Exp Ther* **231:**102–108.
McKay DB and Trent-Sanchez P (1990) Effect of noncompetitive nicotinic receptor blockers on catecholamine release from cultured adrenal chromaffin cells. *Pharmacology* **40:**224–230.
McKay DB, Aronstam RS, and Schneider AS (1985) Interactions of microtubule active agents with nicotinic acetylcholine receptors: relationship to their inhibition of catecholamine secretion by adrenal chromaffin cells. *Mol Pharmacol* **28:**10–16.
McKay DB, Chang C, González-Cestari TF, McKay SB, El-Hajj RA, Bryant DL, Zhu MX, Swaan PW, Arason KM, Pulipaka AB, et al. (2007) Effects of analogs of methyllycaconitine on α3β4 nicotinic receptor-mediated adrenal neurosecretion: pharmacological characterization, computational modeling, and pharmacophore development. *Mol Pharmacol* **71:**1288–1297.
Monod J, Wyman J, and Changeux JP (1965) On the nature of allosteric transitions: a plausible model. *J Mol Biol* **12:**88–118.
Pacheco MA, Pastoor TE, Lukas RJ, and Wecker L (2001) Characterization of human α4β2 neuronal nicotinic receptors stably expressed in SH-EP1 cells. *Neurochem Res* **26:**683–693.
Pan YP, Xu XH, and Wang XL (2003) Galantamine blocks delayed rectifier, but not transient outward potassium current in rat dissociated hippocampal pyramidal neurons. *Neurosci Lett* **336:**37–40.
Quick MW and Lester RAJ (2002) Desensitization of neuronal nicotinic receptors. *J Neurobiol* **53:**457–478.
Sine SM and Taylor P (1982) Local anesthetics and histrionicotoxin are allosteric inhibitors of the acetylcholine receptor. Studies of clonal muscle cells. *J Biol Chem* **257:**8106–8114.
Stauderman KA, Mahaffy LS, Akong M, Veliçelebi G, Chavez-Noriega LE, Crona JH, Johnson EC, Elliott KJ, Gillespie A, Reid RT, et al. (1998) Characterization of human recombinant neuronal nicotinic acetylcholine receptors subunit combinations of α2β4, α3β4 and α4β4 stably expressed in HEK293 cells. *J Pharmacol Exp Ther* **284:**777–789.
Wenger BW, Bryant DL, Boyd RT, and McKay DB (1997) Evidence for spare nicotinic acetylcholine receptors and a β4 subunit in bovine adrenal chromaffin cells: studies using bromoacetylcholine, epibatidine, cytisine, and mAb35. *J Pharmacol Exp Ther* **281:**905–913.
Wess J (2005) Allosteric binding sites on muscarinic acetylcholine receptors. *Mol Pharmacol* **68:**1506–1509.
Wheeler DG, Barrett CF, and Tsien RW (2006) L-type calcium channel ligands block nicotine-induced signaling to CREB by inhibiting nicotinic receptors. *Neuropharmacology* **51:**27–36.
Xiao Y, Meyer EL, Thompson JM, Surin A, Wroblewski J, and Kellar KJ (1998) Rat α3/β4 subtype of neuronal nicotinic acetylcholine receptor stably expressed in a transfected cell line: pharmacology of ligand binding and function. *Mol Pharmacol* **54:**322–333.

Address correspondence to: Dr. Dennis B. McKay, Division of Pharmacology, College of Pharmacy, The Ohio State University, 500 West 12th Ave., Columbus, OH 43210. E-mail: mckay.2@osu.edu